Check for updates

Complex coacervation-based loading and tunable release of a cationic protein from monodisperse glycosaminoglycan microgels†

Carl C. L. Schuurmans,[ab] Anna Abbadessa,‡[a] Mikkel A. Bengtson,[a] Galja Pletikapic,[c] Huseyin Burak Eral,[de] Gijsje Koenderink, [ID][c] Rosalinde Masereeuw,[b] Wim E. Hennink [ID][a] and Tina Vermonden [ID]*[a]

Glycosaminoglycans (GAGs) are of interest for biomedical applications because of their ability to retain proteins (*e.g.* growth factors) involved in cell-to-cell signaling processes. In this study, the potential of GAG-based microgels for protein delivery and their protein release kinetics upon encapsulation in hydrogel scaffolds were investigated. Monodisperse hyaluronic acid methacrylate (HAMA) and chondroitin sulfate methacrylate (CSMA) micro-hydrogel spheres (diameters 500–700 μm), were used to study the absorption of a cationic model protein (lysozyme), microgel (de)swelling, intra-gel lysozyme distribution and its diffusion coefficient in the microgels dispersed in buffers (pH 7.4) of varying ionic strengths. Upon incubation in 20 mM buffer, lysozyme was absorbed up to 3 and 4 mg mg^{-1} dry microspheres for HAMA and CSMA microgels respectively, with loading efficiencies up to 100%. Binding stoichiometries of disaccharide : lysozyme (10.2 : 1 and 7.5 : 1 for HAMA and CSMA, respectively) were similar to those for GAG–lysozyme complex coacervates based on soluble GAGs found in literature. Complex coacervates inside GAG microgels were also formed in buffers of higher ionic strengths as opposed to GAG–lysozyme systems based on soluble GAGs, likely due to increased local anionic charge density in the GAG networks. Binding of cationic lysozyme to the negatively charged microgel networks resulted in deswelling up to a factor 2 in diameter. Lysozyme release from the microgels was dependent on the ionic strength of the buffer and on the number of anionic groups per disaccharide, (1 for HAMA *versus* 2 for CSMA). Lysozyme diffusion coefficients of 0.027 in HAMA and <0.006 μm^2 s^{-1} in CSMA microgels were found in 170 mM buffer (duration of release 14 and 28 days respectively). Fluorescence Recovery After Photobleaching (FRAP) measurements yielded similar trends, although lysozyme diffusion was likely altered due to the negative charges introduced to the protein through the FITC-labeling resulting in weaker protein–matrix interactions. Finally, lysozyme-loaded CSMA microgels were embedded into a thermosensitive hydrogel scaffold. These composite systems showed complete lysozyme release in ~58 days as opposed to only 3 days for GAG-free scaffolds. In conclusion, covalently crosslinked methacrylated GAG hydrogels have potential as controlled release depots for cationic proteins in tissue engineering applications.

[a] *Department of Pharmaceutics, Utrecht Institute for Pharmaceutical Sciences (UIPS), Science for Life, Utrecht University, P.O. Box 80082, 3508 TB Utrecht, The Netherlands. E-mail: T.Vermonden@uu.nl*

[b] *Department of Pharmacology, Utrecht Institute for Pharmaceutical Sciences (UIPS), Science for Life, Utrecht University, P.O. Box 80082, 3508 TB Utrecht, The Netherlands*

[c] *Biological Soft Matter Group, AMOLF, Science Park 102, Amsterdam, 1098 XG, The Netherlands*

[d] *Process and Energy Department, Delft University of Technology, 2628 CD, Delft, The Netherlands*

[e] *Van't Hoff Laboratory for Physical and Colloid Chemistry, Utrecht University, Padualaan 8, 3584 CH Utrecht, The Netherlands*

† Electronic supplementary information (ESI) available: Pictures of free GAG–lysozyme complex coacervation, microfluidic device fabrication, viscosity measurements, FITC–lysozyme uptake experiments, microcomposite and blend hydrogel system confocal images, released lysozyme bioactivity assays and FRAP recovery curves. See DOI: 10.1039/c8sm00686e

‡ Present address: Department of Fibre and Polymer Technology, School of Engineering Sciences in Chemistry, Biotechnology and Health, Royal Institute of Technology, KTH, Teknikringen 56-58, 10044, Stockholm, Sweden.

1. Introduction

Hydrogels are a class of materials under investigation for the controlled delivery of therapeutic protein and as scaffolds for use in tissue engineering.[1–6] In the latter approach, network forming polymers that form hydrogels act as a degradable mimic with similar mechanical properties as the extracellular matrix (ECM) of tissues.[3,7] In natural ECM, sequestration, regulation, and transport of proteins (e.g. growth factors) between cells is mostly controlled by a group of biomacromolecules termed glycosaminoglycans (GAGs). These polysaccharides are negatively charged due to the presence of carboxylate and sulfonate anionic groups. These anionic groups play an important role in electrostatic interactions with cationic residues of proteins, leading to complexation of the protein with the GAG. Such complexes enable retention and regulation of transport of protein.[8,9]

In recent studies, GAG–protein complexation has been utilized in a variety of controlled release delivery systems for proteins. The Schwendeman group for instance, has developed a biomimetic approach based on protein binding biopolymers (e.g. heparin) to increase loading and retard release of cationic proteins from poly(lactic-co-glycolic acid) microparticles.[10,11] Other recent work involves grafting of GAG polymers onto agarose microparticles to absorb and release growth factors.[12] Protein complexation has been exploited previously in order to load protein into covalently crosslinked hydrogels.[13] Also, protein uptake and release from hydrogels that are formed from GAGs that are chemically derivatized with crosslinkable moieties has been shown to occur.[14–17] The ability to 'post-load' proteins into hydrogels in mild environmental conditions allows for high loading efficiencies whilst reducing unwanted protein chemical modification due to e.g. chemical crosslinking.[13,15–19] Therefore, GAGs are promising building blocks for hydrogels capable of sustained release of cationic proteins for use in therapeutic protein delivery and growth factor based tissue engineering.[2–4,7,20–23]

From a physical chemical perspective, GAG–protein complexes can be characterized as complex coacervates (a term originally proposed by Bungenberg-de Jong and Kruyt).[24–26] Complex coacervation is a liquid–liquid phase separation process that can occur when two oppositely charged macromolecules are dispersed in water. Due to electrostatic interaction between the polyanion and polycation, solutions demix into a complex-rich phase (i.e. the coacervate) which is in equilibrium with a complex-poor aqueous phase.[27]

In the present study, two different GAGs, hyaluronic acid (HA) and chondroitin sulfate (CS) were investigated for their applicability in a hydrogel-based depot release formulation of a cationic model protein. Lysozyme was chosen in this study due to its similarity in terms of isoelectric point and molecular weight (pI = 11.4 and mW = 14.3 kDa) to many growth factors.[28–30] HA and CS are structurally related polymers, both consisting of repeating disaccharide units that are composed of alternating glucuronic acids and amino sugars covalently linked by a glycosidic bond.[31,32] In HA, the amino sugar unit consists of N-acetyl glucosamine, whereas in CS the carbon of

the fourth position is epimerized to yield an N-acetyl galactosamine. An important difference between HA and CS, is the partial sulfonation of the hydroxyl groups of CS to yield O-sulfates. Several distinct kinds of sulfated CS exist, each with a different positioning of one or two sulfate groups on the polysaccharide.[33] Both negatively charged HA and CS polysaccharides can form complex coacervates with positively charged proteins.[34] Hydrophilic polymer networks based on HA and CS can be obtained by introduction of e.g. polymerizable methacrylate groups on part of the hydroxyl groups via esterification followed by crosslinking through free-radical polymerization to yield hydrogels.[35–38] Methacrylated hyaluronic acid (HAMA) and methacrylated chondroitin sulfate (CSMA) gels have been studied as carriers for therapeutic proteins and as depots for the controlled release of growth factors.[14,39,40] The focus of research into GAG hydrogels as controlled release depots so far, has been mainly on the biological effects of the released growth factors on cell differentiation and proliferation. However, studies in which the parameters governing protein uptake and release from methacrylated GAG based hydrogels are lacking.

In the present study, we therefore evaluated the potential of methacrylated GAG hydrogels for protein delivery and tunability of protein release kinetics upon encapsulation in hydrogel scaffolds typically used in tissue engineering applications. Since hydrogel depot size uniformity is a key factor in ensuring reproducible protein release kinetics,[41] HAMA and CSMA-based microgels were fabricated through a microfluidic technique. These monodisperse GAG microgels were used for the uptake and controlled release of a positively charged model protein (lysozyme). In particular, the effects of the ionic strength of the medium for loading and release as well as the charge density of the GAG-based hydrogels on complexation and subsequent release were studied. To evaluate the potential applicability of GAG microgels as controlled protein delivery particles in scaffolds for tissue engineering, the microgels were loaded into a synthetic thermo-gelling biodegradable bulk hydrogel scaffold (termed thermogel) that was recently used as a scaffold for cartilage tissue engineering,[42–46] and the lysozyme release kinetics from this composite system were investigated.

2. Experimental methods

2.1. Materials

Chemicals and solvents were purchased from Sigma-Aldrich (Zwijndrecht, The Netherlands) and Biosolve (Valkenswaard, The Netherlands) respectively, unless a different supplier is indicated. All chemicals and solvents were used as received. HA sodium salt (with a M_w of 57 kDa) was acquired from Lifecore Biomedical (Chaska, MN). CS type A sodium salt (from bovine trachea) was found to have a M_n of 27 kDa, 94% mass content and 6% mass content of 354 kDa, as determined via Viscotek gel permeation chromatography (GPC).[38] L-Lactide was obtained from Corbion-Purac (Amsterdam, The Netherlands). Irgacure 2959 was purchased from BASF (Ludwigshaven, Germany) and PEG (10 kDa) was supplied by Merck (Darmstadt, Germany). Fluorescein isothiocyanate (FITC) labeled lysozyme (from hen egg white) was

obtained from Nanocs (New York, USA). Sodium salt form 4-(2-hydroxyethyl)-1-piperazineethanesulfonic acid (HEPES) was acquired from Acros Organics (New Jersey, USA). The lysozyme used was extracted from hen egg white (Lot NR. SLBQ0509V).

2.2. Buffer compositions

Three different buffers were used, all containing 0.02 wt% sodium azide to prevent bacterial growth. A 20 mM HEPES buffer (pH adjusted to 7.4) was used as a low ionic strength buffer. A PBS buffer (pH 7.4) with an ionic strength of 170 mM was used as an isotonic buffer and was used as received from Braun (Melsungen, Germany). This buffer contained the following ions: $[Na^+] = 163.9$ mM, $[Cl^-] = 140.3$ mM, $[HPO_4^{2-}] = 8.7$ mM and $[H_2PO_4^-] = 1.8$ mM. A PBS buffer with higher ionic strength was made by adding NaCl to the PBS buffer mentioned above to reach a total ionic strength of 500 mM. Ionic strength was measured with an cryoscopic osmometer (Osmomat 30, Gonotec) and calculated according to the IUPAC standard.[47]

2.3. Synthesis and characterization of methacrylated glycosaminoglycans

HAMA was synthesized according to a method modified by Abbadessa et al. from the original procedure by Hachet et al.[35,38] CS was methacrylated in dimethylsulfoxide (DMSO) via a recently published method.[48] The degree of methacrylation (DM) for the synthesized HAMA and CSMA was determined using a HPLC method previously developed in our group.[49] In short, 15 mg of polymer or dried microspheres was dissolved overnight at room temperature in 6 mL of aqueous 0.02 M NaOH solution. Next, 1 mL of acetic acid was added and the samples were injected into an Alliance Waters HPLC system equipped with UV-VIS detection (Dual Lambda absorbance, monitoring at 210 nm) and a Sunfire C18 column (column temperature was 50 °C). An isocratic method was used based on eluent consisting of 15 : 85 acetonitrile : MilliQ water (pH 2, adjusted with perchloric acid) with a set flow of 1 mL min^{-1}. Samples were referenced to a calibration curve of known concentrations of methacrylic acid. Concentrations were then calculated to yield the degree of methacrylation (DM), defined as the number of methacrylate groups per 100 disaccharide units.[35,38]

2.4. Synthesis of methacrylated poly[(N-2-hydroxypropyl)-methacrylamide mono/dilactate]-PEG triblock co-polymer

A triblock copolymer consisting of a 10 kDa PEG mid-block flanked by p(HPMAm-lac) thermosensitive outer blocks (referred to further as thermopolymer) was synthesized according to Vermonden et al.[44] To assure gelation at 37 °C, a HPMAm-monolactate : HPMAm-dilactate monomer ratio of 75 : 25 was used in the free radical polymerization initiated by a (PEG-ABCPA)$_n$ macroinititator. This triblock copolymer was further derivatized with methacrylate moieties via esterification of part of the hydroxyl groups of the polymer to allow photopolymerization.[38] M_n and DM were determined by GPC and ^{1}H-NMR (in CDCl$_3$) respectively.[44,45] The DM for the thermopolymer is defined as the percentage of available OH groups on the HPMA-lactate side chains which have been methacrylated.[50]

2.5. Fabrication of microgels with a narrow size distribution using a microfluidic device

HAMA and CSMA microgels with a narrow size distribution were fabricated using a custom built microfluidic device based on co-flowing streams (see Fig. 1 for a schematic representation). More details on device construction are given in the ESI.† To form microgels, HAMA or CSMA (2.5 or 5 wt%, respectively) were dissolved overnight in MilliQ water in addition to 0.5 wt% of Irgacure 2959 and subsequently filtered through a Schott-Duran P1 glass filter (nominal pore size: 100–160 μm) to ensure a solution free of particle contaminants. The viscosities of the different polymer solutions were determined using a rheometer (method and results can be found in the ESI†). The solutions were then loaded into a 1 mL Luer lock syringe (designated as 'water phase' in Fig. 1). For the emulsifying oil phase (depicted in orange in Fig. 1) a solution of surfactant (Span 80, 8 wt%) in light mineral oil was used. The water phase flow was set at 100 μL min^{-1}, with variations in the oil phase flow rate ranging between 1 to 8 mL min^{-1}. The inner diameter of the needle used was 115 μm. The obtained emulsion was collected in a petri-dish partially filled with the oil phase and was subsequently placed at a distance of 5 cm under a UV-lamp (Bluepoint 4 UV lamp, point light source, wavelength range: 300–600 nm, intensity at 5 cm from the waveguide: 80 mW cm^{-2}, Hönle UV technology AG, Germany) and irradiated for 10 min. After crosslinking, a large part of the oil phase was decanted from the dish, and the microgels were collected in 50 mL tubes. To remove the emulsifying oil and surfactant, the microgels were washed three times with 50 mL of tetrahydrofuran (THF). For each washing step, THF was added and the suspension was subsequently vortexed for 30 s. After sedimentation of the dehydrated microgels, the THF supernatant was removed by decanting. The dehydrated microspheres were then re-hydrated in MilliQ water and sieved using a 370 μm mesh size steel filter. The sieving allowed relatively small debris originating from the vortexing steps to be separated from the microgels. Finally, the microgels were washed again with THF similarly as described above to dehydrate them. After this step, removal of solvent was achieved by evaporation overnight under a mild N$_2$ flow to yield dry microspheres.
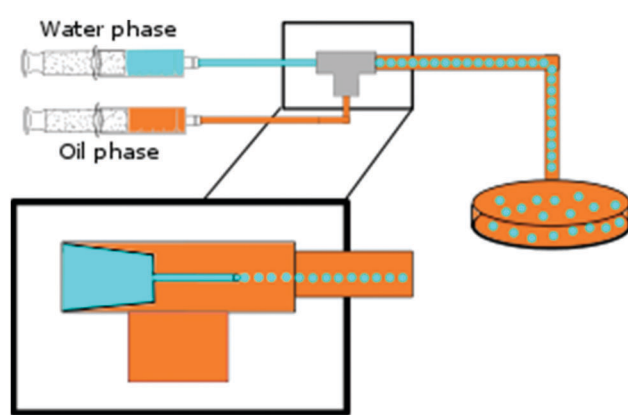

Fig. 1 Schematic representation of a custom-built microfluidic device for generation of monodisperse aqueous HAMA and CSMA droplets.

To determine the methacrylate conversion in microgels, the same method was used as reported for the determination of DM (see Section 2.3).

2.6. Determination of size and size distribution of the microgels

The diameters of the crosslinked HAMA and CSMA microgels were measured using optical microscopy, utilizing a size calibrated Nikon eclipse TE2000-U microscope equipped with a digital camera (Nikon DS-2Mv camera and Nikon DS-U1 digital adapter, with a 4× magnification) and the NIS-elements basic research software package. Pictures of the microgels were taken in different conditions (unloaded, loaded with lysozyme after 1 h and 24 h, and in buffers consisting of 20 and 170 mM ionic strength) and for each gel 3 points on the gel–liquid interface were identified to allow calculation of circular diameter by the program. For each different combination of gel material, loading and buffer, 100 particles were measured. Dispersity of the particles is reported as coefficient of variation (CoV), which is related to the polydispersity index (PDI) and given by eqn (1).[51] The CoV indicates the average percentage difference in diameter between each microgel particle in a batch and is used as a value to convey the narrow size distributions commonly obtained by microfluidic methods for droplet/microgel formation.[52,53]

$$\text{CoV} = \frac{\text{St.D. of microgel diameters}}{\text{Mean microgel diameters}} \times 100 = \sqrt{\text{PDI}} \times 100 \quad (1)$$

For easy visualization, microgels were suspended in 20 mM ionic strength buffer doped with Saffranin-O (0.1 mg mL^{-1}), incubated for 30 min and subsequently washed with 20 mM ionic strength buffer.[54]

2.7. Protein loading of GAG microgels by complex coacervation

To load microgels with lysozyme exploiting complex coacervation, dried microgel samples were weighed (0.50 mg ± 0.05 mg) in separate vials using a precision microgram scale (Mettler-Toledo UMX2, smallest weighable amount = 0.1 µg). All experiments were performed in triplicate. To each vial 450 µL of either 20 or 170 mM ionic strength buffer was added and the gel particles were allowed to swell for 30 min. Subsequently equal volumes of lysozyme (concentrations of 2, 4 and 8 mg mL^{-1}, respectively) in 20 or 170 mM buffer were added and the samples were gently shaken at room temperature. After 1 and 24 hours of incubation, samples were spun down (5300 g for 5 min) and the supernatant was collected. The concentration of lysozyme in the supernatants was quantified using a UPLC method as described earlier.[55] The loading percentage (L) and the loading efficiency (LE) of lysozyme in microgels were calculated respectively according to eqn (2) and (3) as reported previously in similar drug carrier protein uptake studies.[11–13]

$$L\,(\%) = \frac{\text{loaded lysozyme weight}}{\text{dry microgels weight} + \text{loaded lysozyme weight}} \times 100$$
$$(2)$$

$$\text{LE}\,(\%) = \frac{\text{weight of loaded lysozyme}}{\text{weight of added lysozyme}} \times 100 \quad (3)$$

2.8. Preparation of thermogel, GAG/thermogel blends and GAG/thermogel composites for lysozyme release studies

Three types of thermogel-based hydrogels in 20 mM ionic strength buffer were prepared: (A) a thermogel only formulation, in which lysozyme was dissolved (2 mg per 100 µL) into the thermopolymer solution whilst dissolving. (B) A thermogel/CSMA blend, consisting of 0.5 mg of CSMA together with 2.0 mg lysozyme in thermopolymer solution (C) thermogel/CSMA microgel composites were made by weighing 0.5 mg of dry CSMA microspheres that were subsequently loaded with lysozyme for 24 h (lysozyme : CSMA ratio = 4 : 1 w/w) as described in Section 2.7. The protein laden CSMA microgels were then dispersed in 100 µL of thermogel solution and the vial was vortexed for 10 s to facilitate a homogeneous dispersion of CSMA microparticles in the polymer solution.

For all formulations 18 wt% of thermogel was dissolved for 24 h together with 0.05 wt% of Irgacure 2959 in 20 mM HEPES buffer at 4 °C. Next, a solution of 100 µL of the thermopolymer was pipetted into a glass vial with an internal diameter of 5 mm at 4 °C and gellified at 37 °C for 10 min. Gel heights in the vial were ∼4.5 mm. Diffusion of lysozyme from the gel was limited to the upper surface which was in contact with the release buffer. After gelation the formulations were subjected to UV-light for 5 min to induce radical polymerization (using the same lamp as described in Section 2.5, at a distance of 5 cm).

2.9. Confocal fluorescence microscopy of protein up-take and distribution studies using FITC–lysozyme

Protein distribution during loading within microgels, composites and blends was studied using FITC labeled lysozyme and a confocal fluorescence microscope (Yokogawa cell voyager) equipped with a 405 nm laser and a 4× magnification objective. A 1 : 20 FITC–lysozyme : lysozyme (w/w) mixture in 20 mM ionic strength buffer was used. The total concentration of both labeled and unlabeled lysozyme in each mixture was 2 mg mL^{-1}. In a typical experiment, samples of dry microspheres were allowed to swell in 20 mM ionic strength buffer and placed in a well plate. Next, the lysozyme mixture was added to the well in a 4 : 1 protein : microgel w : w ratio (total volume 300 µL) and micrographs of the microgels were taken in 5 min intervals for up to 24 h at room temperature.

2.10. Experimental design, hydrogel groups and methodology of the lysozyme release studies

A total of 9 experimental groups ($n = 3$ for each group) was set-up to monitor the release of lysozyme from the four different types of formulations specified in Table 1. To all formulations (control, blend and composite groups, see Section 2.8) either 900 or 1000 µL (particle groups) of either 170 or 500 mM ionic strength buffer (both with 0.02 wt% sodium azide) were added. The sample temperature during release was 37 °C. Samples of the supernatant (170 µL) were withdrawn at various time-points and replaced with

Table 1 Experimental groups for the release studies

Formulation	Ionic strength of buffer (mM)
HAMA microgels	170
	500
CSMA microgels	170
	500
Thermogel	170
Thermogel/CSMA microgels	170
	500
Thermogel/CSMA blended gel	170
	500

170 µL of fresh buffer to retain a constant volume. All experiments complied with sink conditions (*i.e.* the protein concentration in the supernatant was at least 10 times lower than in the depot at all timepoints). The lysozyme concentrations in the different samples were quantified based on lysozyme's intrinsic fluorescence. A Jasco spectrofluorometer (FP-8300) with a 384 wells-plate reader attachment (FMP-825) was used to quantify fluorescence from release samples *via* interpolation of a measured linear calibration curve of lysozyme in release buffer (5–300 µg mL^{-1}, typical $R^2 > 0.98$). When sample concentrations were found to be outside the linear range, they were diluted accordingly. Neither HAMA nor CSMA were found to exhibit fluorescence in the measured wavelengths, nor were they found to interfere with lysozyme fluorescence. Samples from all time points in each experimental group were measured in triplicate (a volume of 50 µL per single measurement was used). The excitation wavelength was 280 nm and the emission was measured at 340 nm (bandwidth for both excitation and emission was 5 nm).

2.11. Determination of diffusion coefficients of lysozyme from release experiments

Diffusion coefficients of lysozyme in the microgels were calculated from experimental release curves by fitting eqn (4) to the release data. This formula was originally derived by Crank *et al.* to describe Fick-based solute diffusion from a sphere:[56]

$$\frac{M_t}{M_\infty}(t) = 1 - \frac{6}{\pi^2}\sum_{n=1}^{\infty}\frac{1}{n^2}\exp\left(-\frac{Dn^2\pi^2 t}{r^2}\right) \qquad (4)$$

Here, M_t/M_∞ is the normalized fractional release of lysozyme, M_t is the amount of lysozyme released at time t, M_∞ is the total amount of lysozyme released. D is the diffusion coefficient of lysozyme in the microgel matrix in µm^2 s, and r is the average radius of the microgels used in µm.

The diffusion coefficient of lysozyme released from hydrogel scaffolds was calculated using the early time approximation of Fick's second law:[56–58]

$$\frac{M_t}{M_\infty} = 4\sqrt{\frac{Dt}{\pi\delta^2}} \qquad (5)$$

Here, M_t/M_∞ is the normalized fractional release of lysozyme, M_t is the amount of lysozyme released at time t, M_∞ is the total amount of lysozyme released. D is the diffusion coefficient of lysozyme in the gel matrix in µm^2 s and δ represents diffusional distance, which is given by the thickness of the gel in mm.

2.12. Fluorescence recovery after photobleaching (FRAP) of FITC–lysozyme in GAG microgels

The mobility of FITC-labeled lysozyme in GAG microgels consisting of either 5 wt% HAMA or 5 wt% CSMA and dispersed in the buffers mentioned in Section 2.2 was studied using Fluorescence Recovery After Photobleaching (FRAP). GAG microgels were post-loaded in a 20 : 1 lysozyme : FITC–lysozyme weight : weight mixture as specified in Section 2.9 for 24 h. A single microgel for each measurement was then placed in a 200 µm diameter well on a glass slide and 23 µL of either low, isotonic or high ionic strength buffer was added. The system was equilibrated for 30 min before the start of the photobleaching. A circular area of either 10 or 20 µm in diameter in the microgel was bleached for 1 s using an inverted Eclipse Ti microscope (Nikon) equipped with a 488 nm Ar laser (Melles Griot, Alburquerque, New Mexico). The microscope was equipped with 4×, 10×, 20× and 100× objectives. All objectives were used for imaging and the 100× oil immersion objective was used to generate the recovery curves. Laser power was set to minimum ($<0.6\%$) to obtain around 1500 fluorescence (a.u.). The frame interval was set to 0.15 s when using the 100× oil objective. The recovery of the fluorescence after photobleaching was monitored up to 900 s by using a strongly attenuated laser. After normalization, FRAP curves were analyzed using FRAPanalyzer software.[59–61] The FRAP curves were fitted utilizing an equation for a circular bleach area and diffusion-dominated recovery to yield a diffusion coefficient in µm^2 s^{-1} as originally derived by Soumpasis.[62] Corresponding FRAP curves and equations used for normalization and recovery curve fitting are shown in the ESI.†

2.13. Statistical analysis

Sample values are expressed as the mean ± standard deviation (SD) for three independently performed experiments, unless stated otherwise. Statistical analysis was performed using one-way or two-way ANOVA with multiple comparisons by Tukey test in GraphPad Prism 7 (Graphpad Software Inc., California, USA). Kolmogorov–Smirnov and Chi squared goodness of fit tests were performed using the *R* statistical analysis program, where a value of 1 indicates a perfect fit to the experimental data.

3. Results and discussion

3.1. Synthesized materials

Both HA and CS were derivatized with methacrylic moieties with yields of >90% (see Fig. 2A for the chemical structures). Both compounds were obtained as white powder after freeze drying. The DM was 12.6% for HAMA and 11.8% for CSMA. Analysis by Viscotek GPC showed a M_n of 57 kDa for HAMA, CSMA consisted of two populations of chain lengths where 94 wt% had a M_n of 27 kDa and the remaining 6 wt% had a M_n of 354 kDa (in agreement with a previous study).[48] The thermosensitive polymer (thermopolymer, Fig. 2B), was synthesized with similar characteristics and yields as previously described.[38,43,44] GPC analysis showed a M_n for the different batches between 29 and 35 kDa and a DM between 9.5 and 10.1% was determined using
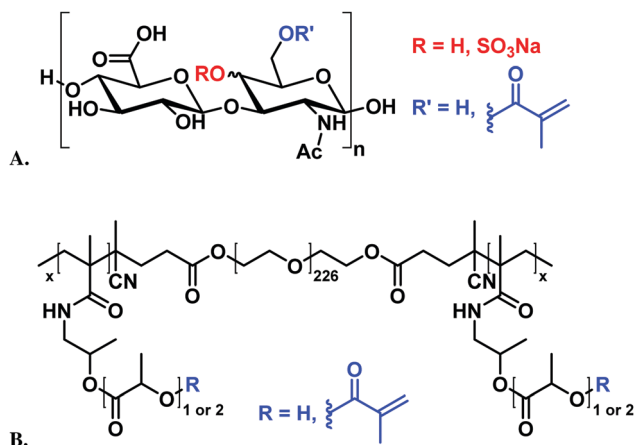
Fig. 2 (A) Chemical structures of HAMA and CSMA type A, R = H or a methacrylate and R′ = H for HAMA, R′ = SO₃Na for CSMA type A. (B) Chemical structure of the thermopolymer used in this study, with a PEG 10 kDa middle block and two thermosensitive p(HPMAm-lac) outer blocks. Methacrylate groups in both structures are indicated in blue.

Table 2 Characteristics of chemically derivatized glycosaminoglycans and thermogel

Polymer	M_n (kDa)	(PDI)	DM in %
HAMA	57[a]	n.d.[b]	12.6[d]
CSMA	27 (94 wt%)[c]	1.4[c]	11.8[d]
	354 (6 wt%)[c]	1.3[c]	
Thermopolymer	29–35[e]	2.0[e]	9.5–10.1[f]

[a] Determined via MALS-SEC as described by the supplier. [b] Not determined. [c] Determined by Viscotek GPC analysis. [d] Determined via the HPLC method, as described in Section 2.3. [e] Determined via GPC analysis according to Vermonden et al.[44] [f] Determined via ¹H-NMR analysis according to Vermonden et al.[45]

¹H-NMR analysis. The ratio of HPMAm-monolactate : HPMAm-dilactate which dictates the hydrophobic/hydrophilic balance and thus the LCST properties of the polymer was between 66 : 34 and 78 : 22 (mol : mol) for different thermopolymer batches synthesized (determined using ¹H-NMR analysis) and was close to the feed ratio of 75 : 25.[44,50,63] The characteristics of the different materials synthesized are summarized in Table 2.

3.2. Microfluidic fabrication of GAG microgels

Aqueous solutions of methacrylated GAGs in the presence of a photoinitiator were used to obtain micrometer sized gels using a microfluidic device based on co-flowing streams of immiscible fluids. Fig. 3A shows that increasing the continuous phase flow at a constant disperse phase flow resulted in a reduction of the diameter of the generated water-in-oil droplets. These results are in line with previous studies of emulsified droplets prepared using co-flowing microfluidic devices.[64] Higher flow rates of the oil phase increase the shear at the nozzle experienced, causing disperse phase droplets to break off from the nozzle faster, reducing the total volume per droplet.[52]

Remarkably, at high continuous phase flow rates the average droplet diameter was smaller than the theoretical limit of 230 μm (indicated by the black line in Fig. 3A), which is defined

as twice the inner diameter of the needle used to inject the aqueous phase into the oil phase.[64,65] The smaller average diameter of the emulsified droplets than the theoretical limit is likely caused by the formation of satellite droplets. These are smaller droplets that typically are formed when droplet generation from viscous solutions transitions from a fluidic dripping regime (where monodisperse droplets are formed) to a dripping with satellites and eventually a jetting regime.[58] The formation of satellites alongside the main droplets leads to two droplet populations varying greatly in diameter (see Fig. 3C and D for micrographs of emulsions with and without satellite droplets). Such a bidisperse distribution of droplet sizes is typical of a dripping with satellites fluidic regime.[58]

The fluidic transition to a dripping with satellites regime and satellite droplet formation can also explain the observed increase of the CoV at higher continuous phase flows (Fig. 3B). Differences in diameters of the different GAG droplets can also be observed: the 5 wt% HAMA droplets increase rapidly in CoV starting at a continuous phase flow of 4 mL min⁻¹ due to produced satellite droplets, whereas the 5 wt% CSMA and 2.5 wt% HAMA droplets had characteristics of dripping with satellites at higher flow rates, i.e. 6 and 8 mL min⁻¹ respectively. The regime changes at different continuous phase flow rates can be explained by the variation in disperse phase fluid viscosity. As reported earlier, higher disperse fluid viscosities increase the propensity for jetting and thus satellite droplet formation.[66] The viscosities of 5 wt% HAMA, 5 wt% CSMA and 2.5 wt% HAMA solutions were 54, 33 and 13 mPa s respectively, indicating that the results obtained here are in line with established theory.[67,68]

Based on the initial screening of droplet and satellite formation a fixed continuous phase flow of 2 mL min⁻¹ was selected for fabrication of the different GAG microgels. In total 10 batches of microgels of both HAMA and CSMA at 2.5 and 5 wt% were made. After UV crosslinking, the GAG microgels were washed and collected as dry particles. These particles were then resuspended in 20 mM ionic strength buffer and stained by Safranin-O to enable easy visualization (see Fig. 4).[54] Fig. 4A shows that the microgels made from the 2.5 wt% CSMA solution were not mechanically stable and fragmented during washing whereas the 5 wt% CSMA microgels (Fig. 4B) did not disintegrate but were too weak to fully retain their original shape. The black circles visible in the microgels are likely air pockets. For the HAMA microgels a similar trend was observed, as the 2.5 wt% HAMA solutions after UV-polymerization yielded spherically shaped gel particles with some debris (Fig. 4C). Moreover, the microgels made from the 5 wt% HAMA solutions exhibited an almost perfect rounded shape fidelity (Fig. 4D). The conversion of methacrylate groups after UV-polymerization for the 2.5 wt% HAMA, 5 wt% HAMA and 5 wt% CSMA was found to be 87, 93 and 90% respectively. The differences in gel cohesion between CSMA and HAMA can partially be explained by the difference in molecular weight of the starting materials (∼26.9 kDa for CSMA and 57 kDa for HAMA). Higher molecular weight polymers are known to form stronger, more cohesive gels than those consisting of a similar concentration made from a lower molecular weight polymer.[69] An additional factor in the observed differences in
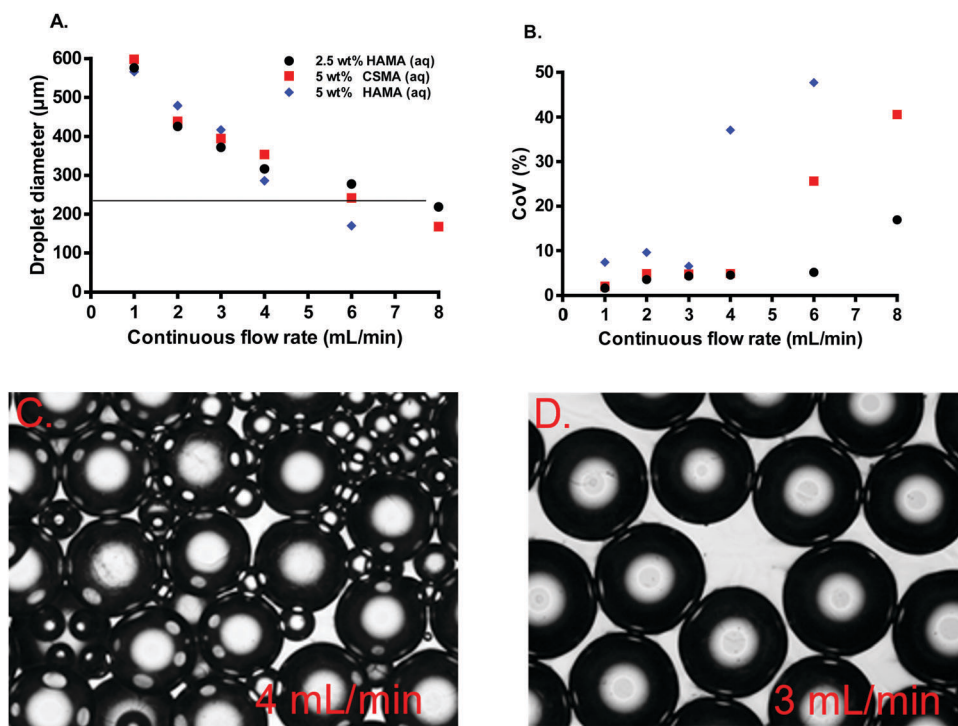
Fig. 3 (A) Diameter and (B) CoV as a function of continuous phase flow rate for GAG containing micro-droplets formed with the microfluidic device. All disperse phase solutions were pumped with a flow rate of 100 μL min^{-1} through a 115 μm nozzle. (C and D) Micrographs of 5 wt% HAMA (aq) in mineral oil, at different continuous phase flows.

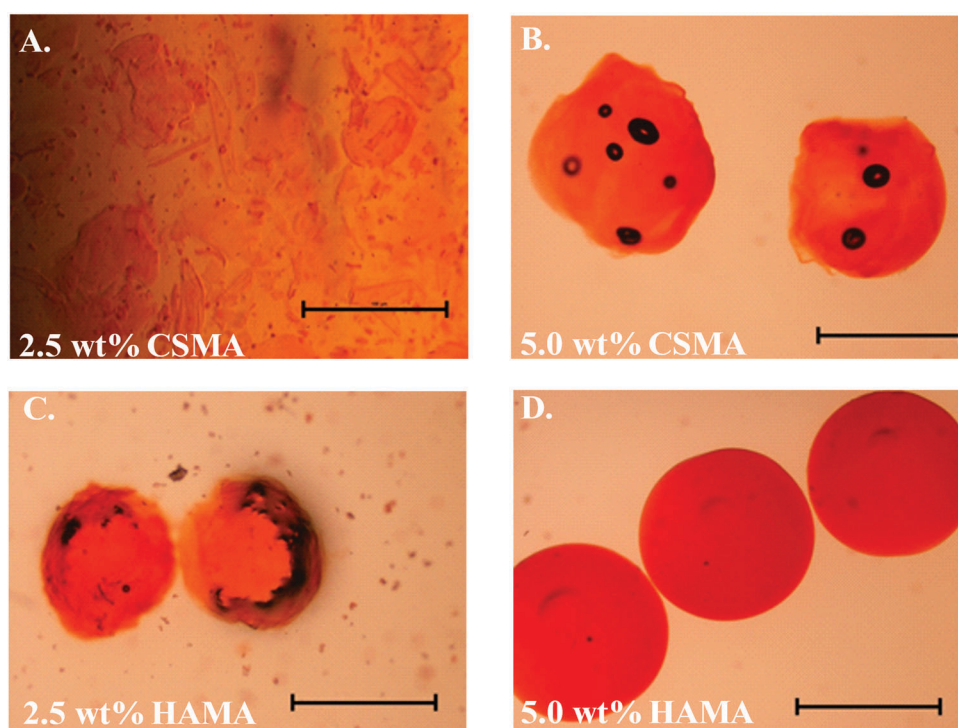**Fig. 4** (A–D) Safranin-O stained GAG microgels made with different wt% aqueous polymer solutions dispersed in 20 mM HEPES (pH 7.4) buffer after washing with THF. The scale bars represent 500 μm.

microgels made from HAMA and CSMA is the charge density of the HAMA and CSMA hydrogel networks. CSMA has a higher charge density then HAMA, which in low ionic strength buffer leads to increased swelling and subsequent higher mechanical stress.

3.3. The effects of buffer ionic strength and incubation time on uptake of lysozyme into GAG microgels *via* coacervation

Complex coacervation of lysozyme with HAMA and CSMA in their soluble form was assessed using a visual turbidity test. The addition of lysozyme to soluble HAMA and CSMA in 20 mM ionic strength buffer resulted in turbid suspensions, indicating complex formation. Addition of lysozyme to HAMA in a 170 mM ionic strength buffer did not result in turbid solutions whereas lysozyme addition to CSMA solutions in the same buffer did result in turbidity. These results demonstrate that lysozyme–HAMA and lysozyme–CSMA coacervation occurs in low ionic strength buffer and that lysozyme–CSMA coacervation can occur in 170 mM ionic strength buffer (method, pictures of the turbid systems due to complexation and more extensive discussion of the results can be found in the ESI†).

The potential of the fabricated GAG microgels to absorb lysozyme through complex coacervation was evaluated by determining the loading (L) and loading efficiency (LE) (eqn (2) and (3)). Fig. 5A shows the lysozyme loading and loading efficiency of GAG microgels in 20 mM ionic strength buffer at a lysozyme : GAG dry weight ratio of 8 : 1. The microgels made from 2.5 and 5 wt% HAMA both exhibited a high loading of $\sim 76\%$ and LE of $\sim 39\%$ after 1 h of incubation and showed no further increase upon incubation for 24 h. Comparatively, the microgels of 5 wt% CSMA showed a loading of 78% and LE of 45% after 1 h and a significantly higher L of 82% (with LE reaching 59%) after 24 h when compared to the HAMA-based microgels. This difference in loading capacity can likely be attributed to the higher number of negative charges per disaccharide unit of CSMA compared to HAMA. HAMA has one carboxylic acid group per disaccharide, whereas the CSMA used in this study has one carboxylic acid group and a sulfate moiety per disaccharide unit (see Fig. 1A).

When expressed in weight/weight, the HAMA microgels took up ~ 3 mg of lysozyme per mg of dry microspheres, whereas the CSMA-based microgels absorbed ~ 4 mg of lysozyme per mg.

In terms of binding stoichiometry, HAMA microgels in low ionic strength buffer show a binding coefficient of ~ 10.2 disaccharide units to 1 lysozyme molecule, very similar to the $\sim 10 : 1$ stoichiometry for free HA polymer–lysozyme complex coacervates reported by both Morfin *et al.* and Waters *et al.*[70,71] The binding stoichiometry of CSMA–lysozyme in the microgels was calculated to be $\sim 7.5 : 1$, similar to the stoichiometries ranging from $6.6 : 1$ to $8 : 1$ as found previously by Moss *et al.* for hen egg white lysozyme complexed with CS immobilized on agarose beads in buffers with ionic strengths ranging between 5 and 60 mM.[72,73]

In a buffer of 170 mM ionic strength some differences were observed in complex coacervation of lysozyme with the GAG microgels (Fig. 5B). The HAMA-based microgels showed a lower loading when incubated in isotonic buffer as compared to the low ionic strength buffer. In detail, in the isotonic buffer, L and LE were 51 and 15% respectively after 1 h. When compared to the low ionic strength buffer, a reduction (from 76% to 51% at $t = 1$ h) in lysozyme loading in both HAMA formulations was observed. This reduction in loading for HAMA formulations is directly related to the increased ion concentration which leads to shielding of the charges on both the microgel matrix as well as the protein.[70–73] Interestingly, the CSMA formulation did not show a significant reduction in loading as compared to the low ionic strength buffer, with a L and LE of 74 and 38% respectively after 1 h and a L and LE of 79 and 48% respectively after 24 h. This difference in loading and complexation due to the effect of ionic strength is similar to what was observed in earlier studies on complex coacervation of lysozyme with free CS/HA. To explain, Moss *et al.* found no complexation of lysozyme with free HA at ionic strengths of 60 mM and higher, whereas the ionic strength at which no CS–lysozyme complex coacervates were detected was around 150 mM.[72] Remarkably, the fabricated HAMA microgels showed loading in solutions with an ionic strength of 170 mM, and the CSMA microgels even showed similar loading in 170 mM ionic strength solutions compared to solutions with
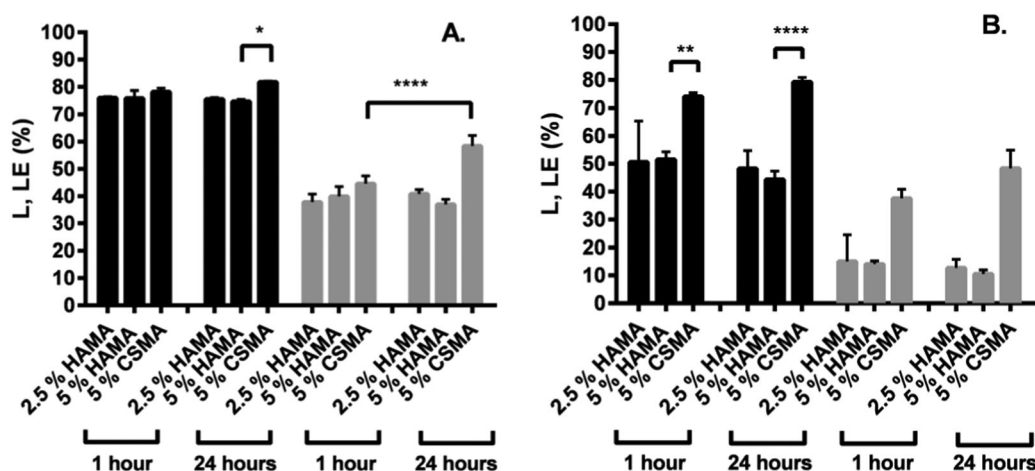

Fig. 5 Loading % (L %, ■) and loading efficiency % (LE %, ▨) of lysozyme in HAMA/CMSA microgels after 1 and 24 h of incubation. (A) Incubation in 20 mM HEPES pH 7.4 with a 8 : 1 w/w feed ratio lysozyme : microgel and (B) incubation in 170 mM PBS pH 7.4 with a 8 : 1 w/w feed ratio lysozyme : microgel, $n = 3$, significant values are marked with an asterisk (* $p < 0.05$, ** $p < 0.01$, **** $p < 0.0001$).
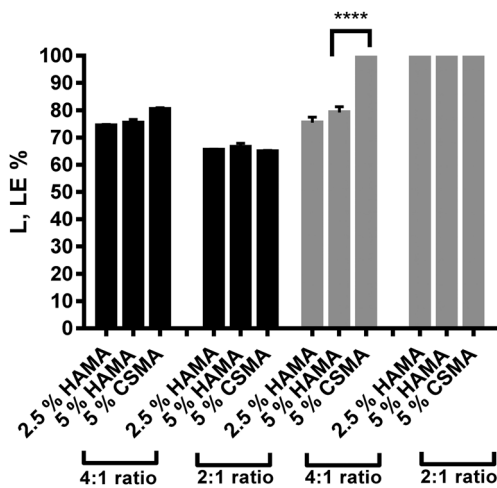
Fig. 6 Loading % (L %, ■) and loading efficiency % (LE %, ■) of lysozyme in GAG microgels using different feed ratios after 24 h of incubation in 20 mM HEPES pH 7.4. $n = 3$, significant values are marked with an asterisk (**** $p < 0.0001$).

a 20 mM ionic strength. A possible explanation for the higher binding strength of the GAG microgels with lysozyme compared to the soluble polymer is that the negatively charged moieties are more densely packed in the hydrogel microparticles as compared to the free polymer in solution, leading to less screening effects of the ions introduced by use of buffers of higher ionic strength.

To study the loading capacities and loading efficiencies of the microgels, loading experiments in low ionic strength buffer at varying protein concentrations were performed (respectively, 4 : 1 and 2 : 1 lysozyme : microgel feed weight ratios). Fig. 6 shows that the HAMA microgels had a L and LE of ~74–76 and 75–80%, respectively after 24 h. CSMA microgels had a L and LE of ~81 and 100%, respectively, which was the same loading as found when the feed ratio was 8 : 1 lysozyme : microgel (Fig. 5A), indicating that above a feed ratio of 4 : 1 saturation of the microgels occurred. For the 2 : 1 lysozyme : microgel weight ratio, the different formulations reached a L of 65–67%, quantitatively removing the lysozyme from solution in the course of the 24 h incubation period (LE = 100%). These exceptionally high LEs demonstrate the strong binding affinities of GAG-based materials with lysozyme in buffer of low ionic strength.

3.4. Effects of protein uptake and ionic strength on GAG microgel swelling

To visualize the kinetics of lysozyme absorption by 5% HAMA and 5% CSMA microgels, a mixture of FITC labeled lysozyme and unlabeled protein was incubated with the microgels. In ESI,† Fig. S2A–D, the lysozyme uptake of 5% HAMA microgels is shown at different time points and both bright field and fluorescence confocal images were taken simultaneously (animated movies can also be found in the ESI† [supplemental Movies 1 and 2]). Lysozyme was found to homogeneously distribute over both GAG microgel types. In the HAMA microgels, the protein was homogeneously distributed after 45 min and no further

uptake of lysozyme was observed after 1 h whereas for the CSMA microgels it took roughly 12 h to absorb (FITC) lysozyme up to their loading capacity (for an extended analysis of FITC–lysozyme absorption into GAG microgels see ESI,† Fig. S2). The incubation of lysozyme with the GAG microgels also led to substantial deswelling. To quantitatively study the effects of the uptake of protein on the swelling of the GAG microgels, their circular diameters were determined when loading lysozyme in a 4 : 1 lysozyme : microgel weight ratio in different ionic strength buffers (20 and 170 mM) after they were swollen to equilibrium. A significant reduction in size was observed when comparing empty microgel size in 170 mM and in 20 mM ionic strength buffer (Fig. 7A–C). This is a well-known effect in polyelectrolyte gels, as an increase in salt concentration leads to shielding of the charges of the networks, which in turn results in less chain–chain electrostatic repulsion and subsequent deswelling.[74]

Fig. 7A–C show the average diameter of three different microgels before and after 1 and 24 h of incubation with 4 mg mL^{-1} lysozyme in the two specified buffers. This figure shows that the diameter of the microgels in 20 mM ionic strength buffer were 500, 640 and 700 μm for 2.5% HAMA, 5% HAMA and 5% CSMA respectively. The original emulsion droplet diameters were 425, 480 and 440 μm for 2.5% HAMA, 5% HAMA and 5% CSMA respectively (Fig. 3A). The differences in size between the microgels in 20 mM ionic strength buffer and the emulsified droplets in oil are mostly related to the charge density of the polymer used. A higher initial charge density (i.e. number of negative charges in the initial droplet) will result in an increased swelling in the formed hydrogel particles due to stronger charge–charge repulsion. The corresponding CoVs of the microgel formulations were 6%, 4% and 18%. A CoV of 18% is equal to a PDI of 0.03 according to eqn (1), showing that the fabricated microgels were almost monodisperse. After 1 h of loading with lysozyme in 20 mM ionic strength buffer, the 2.5% HAMA microgels shrank to half their size (250 μm), with no significant change after 24 h. For the 5% HAMA microgels shrinking was also observed after 1 h with further shrinking to ~400 μm (from the initial size of 640 μm in 20 mM ionic strength buffer) after 24 h of post-loading in 20 mM ionic strength buffer. However, no change in size was observed for the HAMA microgels in 170 mM ionic strength buffer after loading with lysozyme. For CSMA microgels (Fig. 7C) a significant size change was also observed in 20 mM ionic strength during incubation with lysozyme after 1 h from 700 to 490 μm, with no significant change after 24 h. In 170 mM ionic strength buffer, the CSMA microgels shrunk from 570 to 400 μm after 24 h incubation with lysozyme. This deswelling of the microgels is due to the complex coacervation of cationic lysozyme with the HAMA/CSMA, neutralizing their negative charges which in turn results in less charge repulsion of the polymer chains of the network and expulsion of water.[75–77] Interestingly, many studies reported the dehydration of complex coacervate phases consisting of protein and free polyelectrolyte of opposite charge in similar experimental conditions, even leading to precipitation of said complexes in some cases.[78–82] When observing the differences in size, the
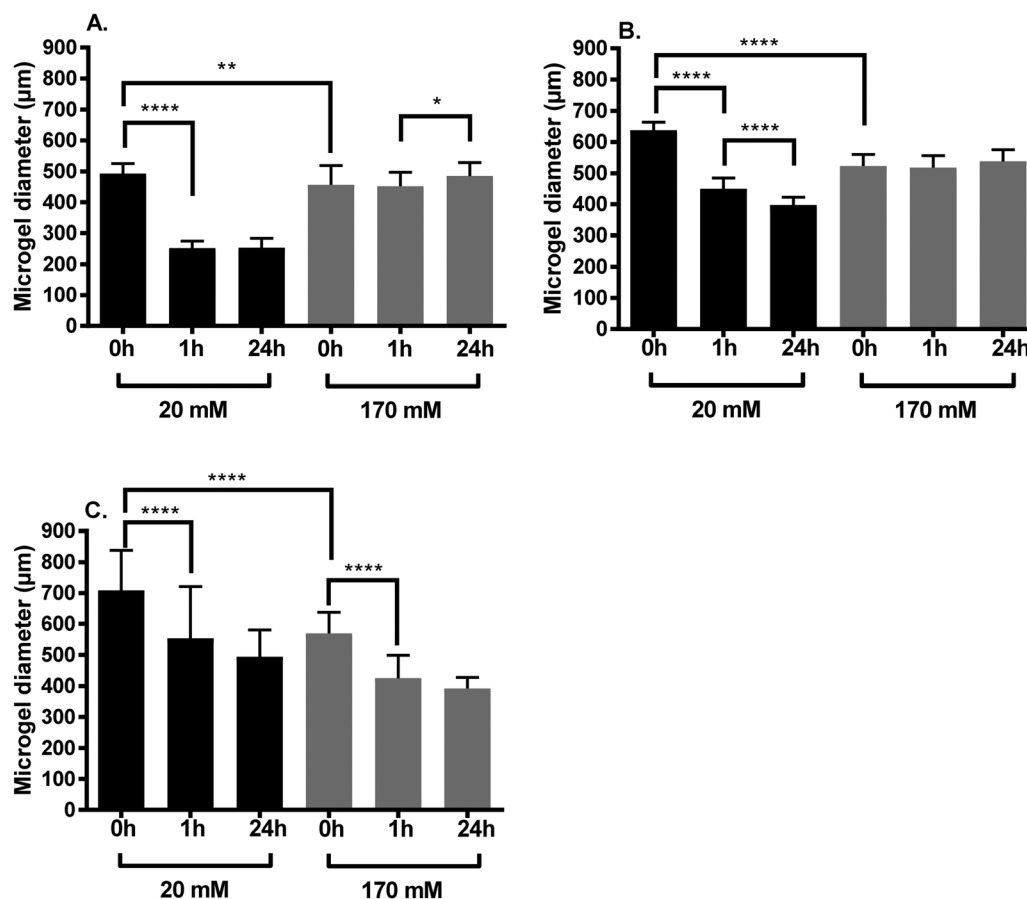
Fig. 7 The size of GAG microgels in 20 mM buffer pH 7.4 (black) and 170 mM buffer pH 7.4 (grey) before and after 1 or 24 h of incubation with lysozyme using a 8 : 1 lysozyme to microgel weight ratio. Graphs A, B and C show the sizes of the 2.5 wt% HAMA, 5 wt% HAMA and 5 wt% CSMA microgels respectively. Significant values are marked with an asterisk (* $p < 0.05$, ** $p < 0.01$, **** $p < 0.0001$).

2.5 wt% HAMA formulation (in 20 mM ionic strength buffer) exhibited the largest relative shrinking upon incubation with lysozyme (a reduction of a factor 2 in diameter). On the other hand, the 5 wt% HAMA microgels in 20 mM buffer showed less dehydration and decreased a factor 1.6 in diameter upon loading with lysozyme. The CSMA microgels in both the 20 and 170 mM buffer shrunk a factor 1.4 in diameter after absorbing lysozyme.

The substantial changes in microgel diameter as a result of protein uptake become most apparent when viewed in terms of volume. Respective reductions in volume of a factor 8, 4 and ∼2.9 for the 2.5% HAMA, 5% HAMA and 5% CSMA formulations were observed. Interestingly, both HAMA formulations only showed deswelling when incubated with lysozyme in the 20 mM buffer. This is possibly due to the reduced loading of lysozyme in 170 mM ionic strength buffer, as compared to the loading in 20 mM ionic strength buffer (as can be seen in Fig. 5A and B). Strikingly, the CSMA formulation shows no such difference in lysozyme loading and shrinking when incubated in buffers of different ionic strength. It is possible that the interaction between the CSMA microgels and lysozyme leads to formation of complex precipitates instead of coacervates in the hydrogel matrix, which could explain the similarities

in lysozyme loading (see Fig. 5A and B) and CSMA microgel diameter after incubation in both 20 and 170 mM (Fig. 7).[78–82]

3.5. *In vitro* release of lysozyme from GAG microgels and FRAP analysis of FITC-labeled lysozyme in GAG microgels

To demonstrate the potential of the fabricated GAG microgels to serve as depots for controlled release of a cationic model protein, the release of lysozyme in a 170 mM PBS buffer with a pH of 7.4 was studied. Furthermore, in order to gather more insights into the release mechanism, release of lysozyme from GAG microgels was also measured in 500 mM ionic strength buffer (pH 7.4). Fig. 8 shows the release of lysozyme from both HAMA (Fig. 8A) and CSMA (Fig. 8B) microgels in the two buffers mentioned.

Fig. 8 shows that the formulations showed no burst release, which can be ascribed to the homogeneous distribution of the lysozyme in the microgel matrices. The release curves were fitted using eqn (4) and these fits were used to calculate the diffusion coefficient of the lysozyme in the microgels (the curves fitting the experimental data according to eqn (4) are represented by the solid lines in Fig. 8A and B). A Chi squared test and the Kolmogorov–Smirnov test (abbreviated as ChiSq and K–S respectively) were used to determine whether the fit describing a Fickian release profile from eqn (4) was descriptive
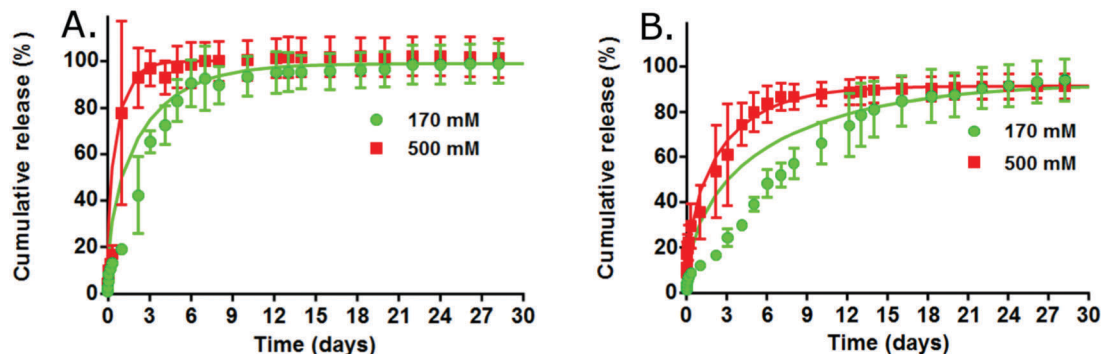
Fig. 8 Release of loaded lysozyme from (A) 5 wt% HAMA microgels and (B) 5 wt% CSMA microgels in release medium of 170 mM (green) and 500 mM (red) ionic strength (pH 7.4). The plotted lines are approximate fits of the data using eqn (4). For all formulations $n = 3$, mean ± SD.

of the experimentally obtained release pattern. In these tests a value of 1 is considered a perfect fit. All formulations showed a nearly quantitative release, showing the potential of GAG-based materials for protein release.

When incubated in the 170 mM ionic strength buffer, lysozyme loaded into 5 wt% HAMA microgels exhibited a diffusion coefficient of 0.027 μm^2 s^{-1} (K–S: 0.86, ChiSq: 0.83). Lysozyme in the HAMA microgels incubated in 500 mM ionic strength buffer had a diffusion coefficient of 0.090 μm^2 s^{-1} (K–S: 0.75, ChiSq: 0.83). For comparison, the diffusion coefficient of lysozyme in buffer is 104 μm^2 s^{-1}.[55] The faster lysozyme release in high ionic strength buffer can be explained by the fact that an increasing salt concentration reduces the strength of the inter- action between the negatively charged hydrogel network and the loaded cationic lysozyme. The release patterns of lysozyme for the CSMA microgels showed the same correlation between ionic strength and lysozyme release rate as for the HAMA formulations. Lysozyme in CSMA microgels incubated in 170 mM ionic strength medium had a diffusion coefficient < 0.006 μm^2 s^{-1}, which indicates a strong interaction of the protein and the matrix. Most formulations showed the typical curve trend of Fickian diffusion. Noteworthy, the fitted release curve of the lysozyme release from CSMA microgels in 170 mM ionic strength did not converge well with the data (K–S: 0.42, ChiSq: 0.35). This indicates that the mechanism of release of this formulation was not predominantly diffusion driven, but instead was likely affected by the electrostatic interactions remaining between the protein and the highly charged polymer network of the microgel, and could further indicate the presence of complex precipitates in the lysozyme-loaded CSMA formulation (as discussed in Section 3.4).[78–82]

As a result of the low goodness of fit, the calculated diffusion coefficient for this formulation is considered only as an upper limit. In contrast, the fitted curve of the lysozyme release from the CSMA microgels incubated at 500 mM ionic strength buffer did converge well with the experimental data and yielded a calculated diffusion coefficient of 0.013 μm^2 s^{-1} (K–S: 0.86, ChiSq: 0.99). Lysozyme diffusion in CSMA is slower as compared to the HAMA microgels, which is likely related to the stronger electrostatic interaction of lysozyme with the higher number of negative charges in the microgel matrix of CSMA. The observed

effects of release buffer ionic strength and network anionic charge density on lysozyme diffusion coefficient are also reflected in the time until a plateau was reached for the different formulations. For HAMA microgels lysozyme was released after around 14 and 7 days in 170 and 500 mM respectively. For the CSMA microgels no further release of lysozyme was observed after around 28 and 13 days in 170 and 500 mM respectively.

The mobility of lysozyme in the polymeric matrices was further investigated by FRAP analysis of FITC–lysozyme loaded HAMA and CSMA microgels in the respective buffers. For HAMA microgels incubated in 20 mM ionic strength buffer the fluorescence recovery of FITC–lysozyme was rapid (i.e. < 180 s), the calculated diffusion coefficient of FITC–lysozyme in HAMA microgels was 1.8 μm^2 s^{-1}. For CSMA microgels the fluorescence recovery was very slow (i.e. > 30 min) in the 20 mM ionic strength buffer and it was not possible to accurately calculate the diffusion coefficient. For both HAMA and CSMA microgels lower diffusion coefficients of FITC–lysozyme were measured when incubated in 170 mM ionic strength buffer when compared to 500 mM ionic strength buffer. For HAMA microgels the diffusion coefficients were 5.0 and 11.0 μm^2 s^{-1} in 170 and 500 mM ionic strength buffer respectively. For CSMA, the diffusion coefficients as compared to the HAMA microgels were considerably lower at 0.5 and 3.5 μm^2 s^{-1} (in 170 and 500 mM ionic strength buffer respectively).

The FITC–lysozyme diffusion coefficients as measured through FRAP analysis differ significantly from those calculated from the release experiments. This is likely due to a reduction in the overall positive charge of lysozyme due to coupling of negatively charged FITC labels (i.e. 2 or 3 FITC labels are reacted to lysine residues per lysozyme, according to the supplier's specification). The net charge of lysozyme is +8 at pH 7.4.[70] Due to coupling of FITC to a lysine residue one positive charge is destroyed whereas one negative charge is introduced. This means that when 2 FITC-labels are introduced, the overall positive charge drops from +8 to +4. This reduction in positive charges very likely leads to less interaction with the negatively charged hydrogel matrix, resulting in a higher diffusion coefficient. This is validated by confocal microscopy over time, where it can be seen that after ~3 hours most FITC–lysozyme has leaked out of the microgels (1 frame = 2.5 min, 2 frames per s, see ESI,† Movie 3).

There was no reduction in the enzymatic activity of released lysozyme after 12 days (as measured with a turbidity-based assay, see ESI,† Fig. S6), showing that the protein retained its structural integrity, as was reported earlier for lysozyme dissociated from soluble HA–lysozyme complex coacervates.[71]

3.6. Controlled release of lysozyme from composites

To evaluate the suitability of methacrylated GAG-based materials for cationic protein retention and controlled release in hydrogel scaffolds for tissue engineering, a study of lysozyme release from three distinct types of scaffold was performed. For all three strategies (see Fig. 9A–C for schematic representations) lysozyme release was studied in 170 and 500 mM ionic strength buffer. A thermosensitive hydrogel based on a partially methacrylated triblock copolymer (abbreviated as 'thermogel') was chosen due to its tunable mechanical and degradation properties.[43,44] The concentration and DM of the thermogel used as the bulk gel were previously optimized for chondrocyte encapsulation.[37] In the GAG-free thermogel (see Fig. 9A for a schematic representation) the loaded lysozyme was released quantitatively within 3 days (Fig. 9D), corresponding to a lysozyme diffusion coefficient of 3.8 μm^2 s^{-1} (calculated with eqn (5)) for this formulation. As a comparison, the lysozyme diffusion coefficient in buffer is 104 μm^2 s^{-1}.[55] The other thermogel formulations contained either methacrylated CSMA polymer complexed with lysozyme (Fig. 9B) or CMSA microgels loaded with lysozyme (Fig. 9C).

Fig. 9D and E show the cumulative release of lysozyme from both CSMA/thermogel composites and blends in 170 and 500 mM ionic strength buffers. Similar to the microgel-only release profiles shown in the previous section, lysozyme release was strongly dependent on the ionic strength of the medium. Complete release of loaded lysozyme from CSMA blends occurred after $\sim$9 days and in the CSMA-based composites after $\sim$21 days in the 500 mM release medium (Fig. 9E). In 170 mM ionic strength buffer, the CSMA-based blends released the loaded lysozyme after $\sim$41 days and the thermogel containing the post-loaded CSMA microgels reached a cumulative release plateau after $\sim$58 days (Fig. 9D). These results also indicated a difference between the release patterns of the composites *versus* the blends, as the blend-based formulations consistently release lysozyme in a shorter timeframe. In the 170 and 500 mM ionic strength buffers the differences are 17 and 11 days respectively. Likely, these differences are related to the increased local charge density and higher lysozyme retention found in the microgels (as observed earlier in Section 3.3).

The bioactivity of released lysozyme from both blends and composites (incubated in 170 mM ionic strength buffer) was measured from samples taken at 12 and 41 days, with both showing similar bioactivities as compared to native lysozyme emphasizing the protein-friendly character of the preparation of the microgels (method and data reported in the ESI,† see Fig. S7).

When comparing the utilities of the composite system to the blend system in potential tissue engineering applications,
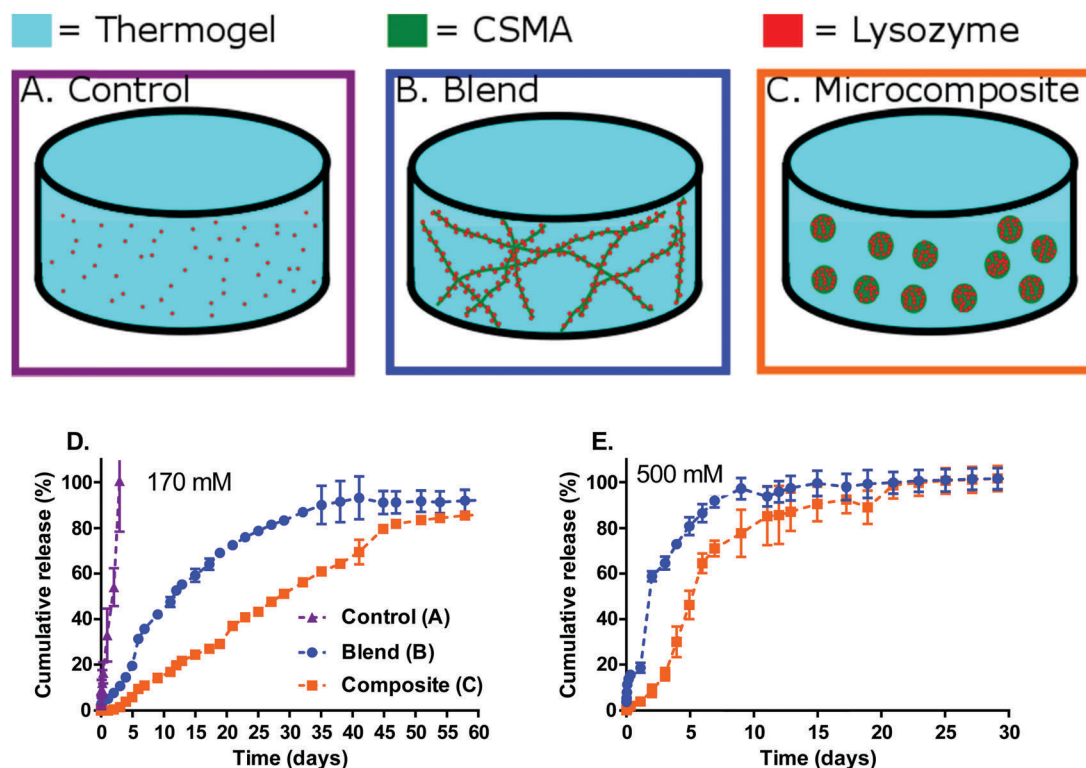

Fig. 9 Lysozyme release from three different formulations. A, B and C depict the control, blend and composite hydrogel formulations respectively (see Section 2.8 for more details). (D) Release of lysozyme in 170 mM ionic strength buffer from the formulations depicted in A, B and C. (E) Release of lysozyme in 500 mM ionic strength from formulations B and C. For all formulations n = 3, results are shown as a mean $\pm$ SD.

a clear advantage of the composite system is found in the capacity of the GAG microgels to temporarily retain protein in isotonic buffer. Additionally, the post-loading technique is superior in avoiding possible protein denaturation/chemical modification when considered against more conventional direct loading techniques were the protein is subjected to free radicals found during crosslinking of the polymer resulting in e.g. oxidation of methionine residues of the protein.[83] The retarded protein release in the microgels in 170 mM ionic strength buffer enables favorable protein release kinetics, allowing more design freedom in terms of tuning the mechanical properties of the bulk hydrogel to better suit the application.

4. Conclusions

HAMA and CSMA-based covalently crosslinked microgels take up lysozyme in 20 mM ionic strength buffer due to complex coacervation, with loading efficiencies up to 100%. Importantly, complex coacervation of lysozyme with HAMA and CSMA microgels was found to also occur in buffer of isotonic ionic strength, in contrast to the soluble polymer GAG–lysozyme complex coacervates reported in literature which dissociate at isotonic ionic strength, indicating an effect of the increased charge density on complex coacervation due to the formation of the hydrogel network. When incubated in a buffer of 170 mM ionic strength, the loaded lysozyme dissociates from the gel matrix and is quantitatively released from the GAG microgels in 7 to 28 days. Curiously, the lysozyme release from CSMA microgels in 170 mM ionic strength buffer was found not to resemble a Fickian release pattern. This phenomenon could be related to the increased electrostatic interactions present, allowing non-diffusion based release kinetics and might indicate the formation of a complex precipitate. This particular effect will be the focus of further work.

Certainly, our results show that coacervation-based post-loading of lysozyme into CSMA microgels or with free CSMA polymer as a blend can significantly retard the release of a cationic protein from a bulk hydrogel which under normal circumstances exhibits fast release of said protein. The post-loading technique utilized in this work is further shown to avoid protein denaturation during loading into the gels, as the protein was found to be fully bioactive after release from all formulations.

As a future perspective; systems based on the complex coacervation mechanisms demonstrated in this research could potentially be used to obtain a gradient release of growth factors, creating cell-specific microenvironments in hydrogel-based scaffolds.

Conflicts of interest

There are no conflicts to declare.

Acknowledgements

References

1 K. Raemdonck, J. Demeester and S. De Smedt, Soft Matter, 2009, 5, 707–715.

2 R. Censi, P. Di Martino, T. Vermonden and W. E. Hennink, J. Controlled Release, 2012, 161, 680–692.

3 B. V. Slaughter, S. S. Khurshid, O. Z. Fisher, A. Khademhosseini and N. A. Peppas, Adv. Mater., 2009, 21, 3307–3329.

4 T. Vermonden, R. Censi and W. E. Hennink, Chem. Rev., 2012, 112, 2853–2888.

5 K. Y. Lee and D. J. Mooney, Chem. Rev., 2001, 101, 1869–1880.

6 Y. Wen, L. Grondahl, M. R. Gallego, L. Jorgensen, E. H. Moller and H. M. Nielsen, Biomacromolecules, 2012, 13, 905–917.

7 N. A. Peppas, J. Z. Hilt, A. Khademhosseini and R. Langer, Adv. Mater., 2006, 18, 1345–1360.

8 J. D. Esko and R. J. Linhardt, Proteins that bind sulfated glycosaminoglycans, Cold Spring Harbor Laboratory Press, Harbor, NY, 2009, ch. 35, pp. 1–12.

9 E. Ruoslahti and Y. Yamaguchi, Cell, 1991, 64, 867–869.

10 S. E. Reinhold, K. G. H. Desai, L. Zhang, K. F. Olsen and S. P. Schwendeman, Angew. Chem., Int. Ed., 2012, 51, 10800–10803.

11 R. B. Shah and S. P. Schwendeman, J. Controlled Release, 2014, 196, 60–70.

12 M. Ansorge, N. Rastig, R. Steinborn, T. König, L. Baumann, S. Möller, M. Schnabelrauch, M. Cross, C. Werner and A. G. Beck-Sickinger, J. Controlled Release, 2016, 224, 59–68.

13 J. P. Schillemans, W. E. Hennink and C. F. van Nostrum, Eur. J. Pharm. Biopharm., 2010, 76, 329–335.

14 J. J. Lim, T. M. Hammoudi, A. M. Bratt-Leal, S. K. Hamilton, K. L. Kepple, N. C. Bloodworth, T. C. McDevitt and J. S. Temenoff, Acta Biomater., 2011, 7, 986–995.

15 M. H. Hettiaratchi, T. Miller, J. S. Temenoff, R. E. Guldberg and T. C. McDevitt, Biomaterials, 2014, 35, 7228–7238.

16 T. E. Rinker, B. D. Philbrick, M. H. Hettiaratchi, D. M. Smalley, T. C. McDevitt and J. S. Temenoff, Acta Biomater., 2017, 68, 125–136.

17 K. M. Park, J. Y. Son, J. H. Choi, I. G. Kim, Y. Lee, J. Y. Lee and K. D. Park, Biomacromolecules, 2014, 15, 1979–1984.

18 A. K. Ekaputra, G. D. Prestwich, S. M. Cool and D. W. Hutmacher, Biomaterials, 2011, 32, 8108–8117.

19 N. Lohmann, L. Schirmer, P. Atallah, E. Wandel, R. A. Ferrer, C. Werner, J. C. Simon, S. Franz and U. Freudenberg, Sci. Transl. Med., 2017, 9.

20 U. Lindahl and M. Hook, Annu. Rev. Biochem., 1978, 47, 385–417.

21 M. C. Koetting, J. T. Peters, S. D. Steichen and N. A. Peppas, Mater. Sci. Eng., R, 2015, 93, 1–49.

22 S. Prokoph, E. Chavakis, K. R. Levental, A. Zieris, U. Freudenberg, S. Dimmeler and C. Werner, *Biomaterials*, 2012, **33**, 4792–4800.

23 K. Chwalek, M. V. Tsurkan, U. Freudenberg and C. Werner, *Sci. Rep.*, 2014, **4**, 4414.

24 B. de Jong, *Proc. R. Acad. Amsterdam*, 1929, **32**, 849–856.

25 A. C. Obermeyer, C. E. Mills, X.-H. Dong, R. J. Flores and B. D. Olsen, *Soft Matter*, 2016, **12**, 3570–3581.

26 C. L. Cooper, P. L. Dubin, A. B. Kayitmazer and S. Turksen, *Curr. Opin. Colloid Interface Sci.*, 2005, **10**, 52–78.

27 C. G. de Kruif, F. Weinbreck and R. de Vries, *Curr. Opin. Colloid Interface Sci.*, 2004, **9**, 340–349.

28 F. Ramirez and D. B. Rifkin, *Matrix Biol.*, 2003, **22**, 101–107.

29 K. Lee, E. A. Silva and D. J. Mooney, *J. R. Soc., Interface*, 2011, **8**, 153–170.

30 R. E. Hileman, J. R. Fromm, J. M. Weiler and R. J. Linhardt, *BioEssays*, 1998, **20**, 156–167.

31 J. Necas, L. Bartosikova, P. Brauner and J. Kolar, *Vet. Med.*, 2008, **53**, 397–411.

32 L. Lapčík, L. Lapčík, S. De Smedt, J. Demeester and P. Chabreček, *Chem. Rev.*, 1998, **98**, 2663–2684.

33 A. Chakrabarti and A. Surolia, *Biochemical Roles of Eukaryotic Cell Surface Macromolecules*, Springer, 2015.

34 X. Du, P. L. Dubin, D. A. Hoagland and L. Sun, *Biomacromolecules*, 2014, **15**, 726–734.

35 E. Hachet, H. Van den Berghe, E. Bayma, M. R. Block and R. Auzély-Velty, *Biomacromolecules*, 2012, **13**, 1818–1827.

36 M. T. Poldervaart, B. Goversen, M. de Ruijter, A. Abbadessa, F. P. Melchels, F. C. Öner, W. J. Dhert, T. Vermonden and J. Alblas, *PLoS One*, 2017, **12**, e0177628.

37 V. H. Mouser, A. Abbadessa, R. Levato, W. Hennink, T. Vermonden, D. Gawlitta and J. Malda, *Biofabrication*, 2017, **9**, 015026.

38 A. Abbadessa, V. H. Mouser, M. M. Blokzijl, D. Gawlitta, W. J. Dhert, W. E. Hennink, J. Malda and T. Vermonden, *Biomacromolecules*, 2016, **17**, 2137–2147.

39 L. Messager, N. Portecop, E. Hachet, V. Lapeyre, I. Pignot-Paintrand, B. Catargi, R. Auzély-Velty and V. Ravaine, *J. Mater. Chem. B*, 2013, **1**, 3369–3379.

40 S. Ansboro, J. S. Hayes, V. Barron, S. Browne, L. Howard, U. Greiser, P. Lalor, F. Shannon, F. P. Barry and A. Pandit, *J. Controlled Release*, 2014, **179**, 42–51.

41 V.-T. Tran, J.-P. Benoît and M.-C. Venier-Julienne, *Int. J. Pharm.*, 2011, **407**, 1–11.

42 A. Abbadessa, M. Landín, E. O. Blenke, W. E. Hennink and T. Vermonden, *Eur. Polym. J.*, 2017, **92**, 13–26.

43 R. Censi, W. Schuurman, J. Malda, G. Di Dato, P. E. Burgisser, W. J. Dhert, C. F. Van Nostrum, P. Di Martino, T. Vermonden and W. E. Hennink, *Adv. Funct. Mater.*, 2011, **21**, 1833–1842.

44 T. Vermonden, N. A. Besseling, M. J. van Steenbergen and W. E. Hennink, *Langmuir*, 2006, **22**, 10180–10184.

45 T. Vermonden, N. E. Fedorovich, D. van Geemen, J. Alblas, C. F. van Nostrum, W. J. Dhert and W. E. Hennink, *Biomacromolecules*, 2008, **9**, 919–926.

46 R. Censi, T. Vermonden, H. Deschout, K. Braeckmans, P. di Martino, S. C. De Smedt, C. F. van Nostrum and W. E. Hennink, *Biomacromolecules*, 2010, **11**, 2143–2151.

47 A. D. McNaught and A. D. McNaught, *Compendium of Chemical Terminology*, Blackwell Science, Oxford, 1997.

48 A. Abbadessa, M. Blokzijl, V. Mouser, P. Marica, J. Malda, W. Hennink and T. Vermonden, *Carbohydr. Polym.*, 2016, **149**, 163–174.

49 R. J. H. Stenekes and W. E. Hennink, *Polymer*, 2000, **41**, 5563–5569.

50 O. Soga, C. F. van Nostrum, A. Ramzi, T. Visser, F. Soulimani, P. M. Frederik, P. H. H. Bomans and W. E. Hennink, *Langmuir*, 2004, **20**, 9388–9395.

51 N. J. Salkind, *Encyclopedia of Research Design*, Sage, 2010.

52 C. Cramer, P. Fischer and E. J. Windhab, *Chem. Eng. Sci.*, 2004, **59**, 3045–3058.

53 I. Ziemecka, V. van Steijn, G. J. Koper, M. Rosso, A. M. Brizard, J. H. van Esch and M. T. Kreutzer, *Lab Chip*, 2011, **11**, 620–624.

54 L. Rosenberg, *J. Bone Jt. Surg.*, 1971, **53**, 69–82.

55 R. Censi, T. Vermonden, M. J. van Steenbergen, H. Deschout, K. Braeckmans, S. C. De Smedt, C. F. van Nostrum, P. Di Martino and W. Hennink, *J. Controlled Release*, 2009, **140**, 230–236.

56 J. Crank, *The Mathematics of Diffusion*, Oxford University press, 1979.

57 P. L. Ritger and N. A. Peppas, *J. Controlled Release*, 1987, **5**, 23–36.

58 P. L. Ritger and N. A. Peppas, *J. Controlled Release*, 1987, **5**, 37–42.

59 A. Halavatyi, S. Medves, C. Hoffman, V. Apanasovich, M. Yatskou and E. Friederich, *Proceedings of FEBS/ECF workshop*, Potsdam, Germany, 2008.

60 T. K. L. Meyvis, S. C. De Smedt, P. Van Oostveldt and J. Demeester, *Pharm. Res.*, 1999, **16**, 1153–1162.

61 H. Deschout, K. Raemdonck, J. Demeester, S. C. De Smedt and K. Braeckmans, *Pharm. Res.*, 2014, **31**, 255–270.

62 D. M. Soumpasis, *Biophys. J.*, 1983, **41**, 95–97.

63 O. Soga, C. F. van Nostrum and W. E. Hennink, *Biomacromolecules*, 2004, **5**, 818–821.

64 P. Umbanhowar, V. Prasad and D. Weitz, *Langmuir*, 2000, **16**, 347–351.

65 H. B. Eral, E. R. Safai, B. Keshavarz, J. J. Kim, J. Lee and P. S. Doyle, *Langmuir*, 2016, **32**, 7198–7209.

66 A. S. Utada, A. Fernandez-Nieves, H. A. Stone and D. A. Weitz, *Phys. Rev. Lett.*, 2007, **99**, 094502.

67 H. A. Stone and S. Kim, *AIChE J.*, 2001, **47**, 1250–1254.

68 A. U. Chen, P. K. Notz and O. A. Basaran, *Phys. Rev. Lett.*, 2002, **88**, 174501.

69 K. Draget, G. S. Bræk and O. Smidsrød, *Carbohydr. Polym.*, 1994, **25**, 31–38.

70 I. Morfin, E. Buhler, F. Cousin, I. Grillo and F. Boué, *Biomacromolecules*, 2011, **12**, 859–870.

71 J. J. Water, M. M. Schack, A. Velazquez-Campoy, M. J. Maltesen, M. van de Weert and L. Jorgensen, *Eur. J. Pharm. Biopharm.*, 2014, **88**, 325–331.

72 J. M. Moss, M.-P. I. Van Damme, W. H. Murphy and B. N. Preston, *Arch. Biochem. Biophys.*, 1997, **348**, 49–55.

73 M. Vandamme, J. Moss, W. Murphy and B. Preston, *Arch. Biochem. Biophys.*, 1994, **310**, 16–24.

74 R. Rydzewski, *Continuum Mech. Thermodyn.*, 1990, **2**, 77–97.

75 Y. Li, R. d. Vries, M. Kleijn, T. Slaghek, J. Timmermans, M. C. Stuart and W. Norde, *Biomacromolecules*, 2010, **11**, 1754–1762.

76 L. Zhao, Y. Chen, W. Li, M. Lu, S. Wang, X. Chen, M. Shi, J. Wu, Q. Yuan and Y. Li, *Carbohydr. Polym.*, 2015, **121**, 276–283.

77 C. Johansson, P. Hansson and M. Malmsten, *J. Colloid Interface Sci.*, 2007, **316**, 350–359.

78 K. Kaibara, T. Okazaki, H. Bohidar and P. Dubin, *Biomacromolecules*, 2000, **1**, 100–107.

79 E. Kizilay, A. B. Kayitmazer and P. L. Dubin, *Adv. Colloid Interface Sci.*, 2011, **167**, 24–37.

80 F. Comert and P. L. Dubin, *Adv. Colloid Interface Sci.*, 2017, **239**, 213–217.

81 F. Comert, A. J. Malanowski, F. Azarikia and P. L. Dubin, *Soft Matter*, 2016, **12**, 4154–4161.

82 J. Van der Gucht, E. Spruijt, M. Lemmers and M. A. C. Stuart, *J. Colloid Interface Sci.*, 2011, **361**, 407–422.

83 J. A. Cadée, M. J. van Steenbergen, C. Versluis, A. J. R. Heck, W. J. M. Underberg, W. den Otter, W. Jiskoot and W. E. Hennink, *Pharm. Res.*, 2001, **18**, 1461–1467.